

[REDACTED] 434

**R E P O R T . P .**

No 1409/IA/PL

**NUCLEAR LEVELS OF  $^{228}\text{Th}$  POPULATED  
IN THE DECAY OF  $^{228}\text{Pa}$**

W. KURCEWICZ  
K. STRYCNIEWICZ  
J. ZYLICZ  
R. BRODA  
S. CHOJNACKI  
W. WALUŚ  
I. YUTLANDOV

SUBMITTED FOR PUBLICATION  
IN JOURNAL DE PHYSIQUE

**WARSZAWA**

**1972**

This report has been reproduced directly from  
the best available copy

Распространяет:  
ИНФОРМАЦИОННЫЙ ЦЕНТР ПО ЯДЕРНОЙ ЭНЕРГИИ  
при Уполномоченном Правительства ПНР  
по Использованию Ядерной Энергии  
Дворец Культуры и Науки  
Варшава, ПОЛЬША

Available from:  
NUCLEAR ENERGY INFORMATION CENTER  
of the Polish Government Commissioner for Use  
of Nuclear Energy  
Palace of Culture and Science  
Warsaw, POLAND

Drukuje i rozprowadza:  
OŚRODEK INFORMACJI O ENERGII JĄDROWEJ  
Pomocnika Rządu d/s Wykorzystania Energii Jądrowej  
Warszawa, Pałac Kultury i Nauki

W y d a j e Instytut Badań Jądrowych

---

Nakład 550 egz., Objętość ark. wyd. 2,04 . Ark. druk 2,94 , Data  
złożenia maszynopisu przez autora 6 VI 72 , Oddano do druku  
24 VI 72 . Druk ukończono VII 72 r. , SP-09/200/66, Zam. nr 219/72

INSTITUTE OF NUCLEAR RESEARCH

NUCLEAR LEVELS OF  $^{228}\text{Th}$   
POPULATED IN THE DECAY OF  $^{228}\text{Pa}$

POZIOMY JĄDROWE  $^{228}\text{Th}$   
ZASILANE W ROZPADZIE  $^{228}\text{Pa}$

УРОВНИ  $^{228}\text{Th}$  ВОЗБУЖДЕННЫЕ  
ПРИ РАСПАДЕ  $^{228}\text{Pa}$

Wiktor Kurcewicz .  
Kamila Stryczniewicz  
Jan Zylicz  
Rafał Broda<sup>\*/</sup>  
Sławomir Chojnacki<sup>\*\*/</sup>  
Władysław Waluś<sup>\*\*\*</sup>  
Igor Yutlandov<sup>\*\*\*\*</sup> /

---

\* / Institute of Nuclear Physics, Cracow, Poland.

\*\* / Institute of Experimental Physics, Warsaw University,  
Warsaw, Poland.

\*\*\* / Institute of Physics, Jagiellonian University, Cracow,  
Poland.

\*\*\*\* / Joint Institute of Nuclear Research, Dubna, USSR.

### Abstract

The decay of  $^{228}\text{Pa}$  to the levels of  $^{228}\text{Th}$  has been extensively studied by various techniques. Singles spectra of  $\gamma$  - and K X-rays have been measured with Si/Li/ and Ge/Li/ detectors. A set of two Ge/Li/ detectors has been used to study  $\gamma$  -  $\gamma$  and  $\gamma$  - K X-ray coincidences. Measurements of  $\gamma$  -spectra in coincidence with the selected internal-conversion lines have been carried out using a Ge/Li/ detector and a six-gap magnetic  $\beta$  -spectrometer. Finally, spectra of internal-conversion electrons have been studied in a  $\beta$  -spectrometer which uses a Si/Li/ detector placed together with a system of diaphragms in a homogeneous magnetic field. The decay scheme has been constructed including 39 levels of  $^{228}\text{Th}$ . It accounts for 111 of 160 transitions ascribed to the  $^{228}\text{Pa}$  activity. The electron-capture decay energy has been determined to be  $2103 \pm 16$  keV. The strength distribution for the electron-capture feeding of the  $^{228}\text{Th}$  levels is analysed in terms of nuclear models. The Coriolis mixing of four octupole bands ( $K = 0, 1, 2$  and  $3$ ) is studied in some detail. The coupling matrix elements deduced from the experiment are compared with the results of the microscopic-model calculations. (auth)

### Streszczenie

Badano rozpad  $^{228}\text{Pa}$  do poziomów  $^{228}\text{Th}$  stosując różnorodne techniki. Pomiar widm prostych  $\gamma$  i promieniowania KX przeprowadzono używając detektorów Ge/Li/ i Si/Li/. W pomiarach koincydencyjnych  $\gamma$  -  $\gamma$  i  $\gamma$  - KX stosowano dwa detektory Ge/Li/. Pomiar widm  $\gamma$  w koincydencji z wy-

branymi liniami elektronów wewnętrznej konwersji przeprowadzono używając detektora Ge/Li/ i sześcioczcielnego magnetycznego spektrometru  $\beta$ . Pomiarów prostego skema elektronów wewnętrznej konwersji przeprowadzono przy użyciu spektrometru  $\beta$  z detektorem Si/Li/ umieszczonym z systemem ruchomych diafragm w jednorodnym polu magnetycznym. Zaproponowano schemat rozpadu zawierający 39 poziomów wzbudzonych  $^{228}\text{Th}$ . Z całkowitej liczby 160 przejść przypisanych do rozpadu  $^{228}\text{Pa}$  w schemacie tym umieszczono 111 przejść. Wyznaczono energię przejścia  $^{228}\text{Pa} \rightarrow ^{228}\text{Th}$ , która wynosi  $2103 \pm 16 - 12$  keV. W oparciu o modele jądrowe przeanalizowano rozkład funkcji mocy dla zasilai poziomów  $^{228}\text{Th}$  na drodze wychwytu elektronu. Przedstawiono analizę oddziaływania Coriolisa pomiędzy pasmami oktopolowymi  $K = 0, 1, 2$  i  $3$ . Doświadczalne wartości elementów macierzowych oddziaływania Coriolisa porównano z wartościami obliczonymi w oparciu o mikroskopowy model jądra.

#### АННОТАЦИЯ

Распад  $^{228}\text{Pa} \rightarrow ^{228}\text{Th}$ , исследовался с применением нескольких методов. Спектры гамма и КХ-лучей изучались с помощью Ge(Li) и Si(Li)-детекторов. Измерения гамма-гамма и гамма-КХ совпадений проводились на установке с двумя Ge(Li) - детекторами. Электрон - гамма совпадения изучались с помощью шестизазорного бета-спектрометра и Ge(Li)- детектора. Спектр конверсионных электронов исследовался на бета-спектрометре с Si(Li) - детектором находящимся, вместе с подвижными диафрагмами, в области однородного магнитного поля. Предлагается схема распада  $^{228}\text{Pa} \rightarrow ^{228}\text{Th}$ , в которой введены 39 уровней. В схеме

размещено 111 гамма-переходов из полного числа 160 гамма-переходов наблюдавшихся при распаде  $^{228}\text{Ra}$ . Определено энергия распада  $^{228}\text{Ra} \rightarrow ^{228}\text{Th}$ , которая равна  $(2103_{-12}^{+16})\text{кэВ}$ .

Экспериментальное распределение силовой функции электронного захвата сравнивается с теоретическими расчетами. Представлен анализ взаимодействия Кориолиса четырех октупольных полос ( $K = 0, 1, 2$  и  $3$ ).

Полученные экспериментальные величины матричных элементов взаимодействия Кориолиса сравниваются с теоретическими расчетами в рамках микроскопической модели ядра.

## 1. INTRODUCTION

Many features of the  $^{228}\text{Pa} \rightarrow ^{228}\text{Th}$  decay scheme were established and discussed by Arbmam et al. [1] already in 1960. However, a decade later the available experimental techniques were much improved, mostly owing to the development of semiconductor detectors, and it seemed reasonable to reinvestigate this decay. The present paper describes such new extensive studies which led to a more complete knowledge of properties of the  $^{228}\text{Th}$  levels. Among other results, the existence of  $K = 0, 2$  and  $3$  octupole bands is confirmed and evidence is given tentatively for the previously unobserved  $K = 1$  octupole band. The Coriolis coupling of these bands is analysed in some detail, reference being made to the microscopic-model calculations. Also the  $^{229}\text{Pa}$  decay energy and branching ratios for the electron-capture feeding of the  $^{228}\text{Th}$  levels are determined, which allows to calculate the distribution of the beta strength and to study this distribution in terms of nuclear models.

## 2. SOURCE PREPARATION

The  $^{228}\text{Pa}$  22 h activity was produced in the  $^{232}\text{Th}(p,5n)$  reaction. About 1 g of metallic thorium foil was bombarded for 3 to 6 hours with 100 MeV protons in the JINR synchrocyclotron at Dubna. Protactinium samples were prepared by the chemical procedure briefly described by Kurcewicz et al. [2]. During the measurements, apart from the  $^{228}\text{Pa}$  activity and traces of its decay products, contributions from  $^{229}\text{Pa}$ ,  $^{230}\text{Pa}$ ,  $^{232}\text{Pa}$  and  $^{233}\text{Pa}$  were observed.

### 3. SINGLES SPECTRA OF $\gamma$ -RAYS AND INTERNAL-CONVERSION ELECTRONS

The low-energy part of the  $\gamma$ -ray spectrum was measured with a 2.5 mm thick and 5 mm in diameter Si/Li/ detector, having at 60 keV a resolution (FWHM) of 1.4 keV. The energy and intensity calibration was performed using the  $^{57}\text{Co}$ ,  $^{109}\text{Cd}$ ,  $^{169}\text{Yb}$  and  $^{241}\text{Am}$  sources.

The spectrum in the energy range of 100 to 2100 keV was measured with several Ge/Li/ detectors. The main results were obtained using a 5.6 cm<sup>3</sup> detector with a 1600 channel analyzer and a 33 cm<sup>3</sup> detector with a 4096 channel analyzer (Fig. 1). The resolution (FWHM) of these detectors at 1332 keV was 3.0 and 4.0 keV, respectively. Energies of the intense  $\gamma$ -lines were determined from those of the standard lines by counting the  $^{228}\text{Pa}$  source and standard sources simultaneously. In several runs, different sets of  $^{22}\text{Na}$ ,  $^{60}\text{Co}$ ,  $^{88}\text{Y}$ ,  $^{110m}\text{Ag}$ ,  $^{207}\text{Bi}$  or  $^{226}\text{Ra}$  standard sources were used. Also the energies of  $\gamma$ -lines of  $^{230}\text{Pa}$  /Kurcewicz et al. [2]/,  $^{232}\text{Pa}$  /Kaczarowski et al. [3]/ and  $^{233}\text{Pa}$  were used as internal-calibration standards. The energies of  $^{228}\text{Pa}$  lines with the assigned uncertainties of 0.2 keV or less were determined in this way. In the next step, these precisely determined energies were considered as secondary standards when finding the energies of weaker lines. For calibrating the efficiency of the detectors such sources as  $^{56}\text{Co}$ ,  $^{110m}\text{Ag}$  and  $^{226}\text{Ra}$  were used, which have several  $\gamma$ -lines with relative intensities accurately known. The intensity of some  $^{228}\text{Pa}$  lines had to be corrected for the contribution from  $\gamma$ -lines of  $^{230}\text{Pa}$ ,  $^{232}\text{Pa}$  or  $^{233}\text{Pa}$ . Some of the  $\gamma$ -spectra were analysed using the GIER computer code.



The energy and intensity data for  $\gamma$ -rays of  $^{228}\text{Pa}$  are listed in columns 1 and 2 of Table I.

Column 3 of Table I lists the data on relative intensities of the lines of internal-conversion electrons. A  $\beta$ -spectrometer with a 3 mm thick Si/Li/detector in a homogeneous magnetic field, described by Plochocki et al. [4], was used for detection of these lines in the energy range above 300 keV. A part of this spectrum is shown in Fig. 2. Since the detector was not thick enough to stop high-energy electrons completely, it was necessary to correct the line intensities for the detection efficiency. The efficiency curve was based on the data reported by Amov et al. [5] who studied the most intense  $^{228}\text{Pa}$  conversion lines, in the energy range above 800 keV, using a high-resolution magnetic  $\beta$ -spectrometer.

To calculate the internal-conversion coefficients, the  $\gamma$ -ray and conversion-line intensities were normalized by assuming the theoretical /Hager and Seltzer [6]/ E2 internal-conversion coefficient of  $6.9 \times 10^{-3}$  for the 911.23 keV transition. The columns 4 and 5 in Table I list, respectively, the values of the internal-conversion coefficients and the multipolarity assignments, deduced by comparing these values with the theoretical ones [6].

#### 4. COINCIDENCE MEASUREMENTS

The  $\gamma$ -spectra in coincidence with internal-conversion electrons were measured using a 5.6 cm<sup>3</sup> Ge/Li/detector and a six-gap magnetic  $\beta$ -spectrometer. The conditions of these measurements were identical to those in  $^{230}\text{Pa}$  studies of Kurcewicz et al. [2]. The results are presented in Table II and, for one of the two coincidence experiments, in Fig. 3.

The measurements of  $\gamma$ - $\gamma$  coincidences were performed using a spectrometer with two Ge/Li/ detectors. These detectors were placed at an angle of about  $60^\circ$  with regard to the source position. Absorbers were used to stop  $\gamma$ -rays scattered from one detector in the direction of the other one. A fast-slow coincidence circuit with a time-to-amplitude converter was applied. Two coincidence spectra were recorded simultaneously. One was gated by a selected  $\gamma$ -line and a portion of the Compton continuum, and the second one by a section of this continuum above the line. Thus the pure coincidence effect due to the selected transition could be deduced. In Fig. 4 a typical pair of coincidence spectra is shown by way of example. As it may be seen from Table II, the coincidence data were obtained for five gating lines.

##### 5. DETERMINATION OF THE ELECTRON-CAPTURE DECAY ENERGY

The method used to determine the  $^{228}\text{Pa}$  decay energy  $Q_{EC}$  was similar to that described by Kurocwiec et al. [2] for the decay of  $^{230}\text{Pa}$ . It takes account of the well known dependence of the relative K-capture probability  $P_K$  upon the electron-capture transition energy  $Q$ .

The ratio of the intensities was determined experimentally for the 1538 and 1887 keV  $\gamma$ -lines from the singles  $\gamma$ -ray spectrum and the spectrum coincident with the K X-rays (cf. Fig. 5). From these data it was possible to calculate the ratio of the  $P_K$  values for the electron-capture transitions to the levels at 1646 and 1945 keV (cf. Fig. 6). This ratio was found to be  $0.47 \pm 0.11$ , where from the energy for the transition to the 1945 keV level is equal to  $159 \pm 16$  keV.

Thus, the decay energy is  $Q_{EC} = 2103 \pm 16$  keV.

## 6. THE DECAY SCHEME

The  $^{228}\text{Pa}$  decay scheme shown in Figs. 7a and 7b is an extension of that published by Arberman et al. [1]. The twenty one levels of  $^{228}\text{Th}$  reported in Ref. [1] have been confirmed, and new levels at 618, 952, 969 ( $2^-$ ), 1016, 1064, 1175, 1200, 1580, 1642, 1676, 1843, 1900, 1925, 1939, 1965, 1994, 2010 and 2016 keV have been found. It has recently been shown that many of these new levels are populated also in the  $\beta^-$ -decay of  $^{228}\text{Ac}$  /Dalmasso and Maria [7], Herment and Vien [8]/.

The construction of the  $^{228}\text{Th}$  level scheme is based on the transition energy fits, searched with the use of a special computer program, and on the results of the coincidence experiments. The decay scheme includes 111 of the total number of 160 transitions ascribed to the  $^{228}\text{Pa}$  activity. The multipole character established for numerous transitions allows to define the parity for the majority of the  $^{228}\text{Th}$  levels and to assign spin values to many of them. With the knowledge of the  $Q_{\text{EC}}$  value, of the  $^{228}\text{Pa}$  half-life and of the EC branching ratios it was possible to calculate  $\log ft$  values. The low  $\log ft$  value for the transition to the 1944 keV  $3^+$  level and the direct  $\alpha$  feeding of the  $2^+$  and  $4^+$  levels indicates the spin and parity  $3^+$  for the  $^{228}\text{Pa}$  ground state. This is in agreement with the assignment proposed by Arberman et al. [1]. The assignments of the K quantum numbers to the levels at lower excitation energy results from the interpretation of these levels in terms of nuclear models (cf. section 7).

The arguments taken into account when constructing the decay scheme can be easily reproduced if use is made of the information contained in Tables I - III. It has

been decided, therefore, to omit in this section any comments on the existence of individual levels in  $^{228}\text{Th}$  and on the spin-parity assignment. In the next section, however, brief comments can be found on several, mostly tentative, levels whose identification is important for the verification of the applicability of the deformed-nuclei theory to the low-energy excitations in  $^{228}\text{Th}$ .

The balance of the intensities for the decay scheme is based on the assumption that the EC process occurs in 98% of the  $^{228}\text{Pa}$  decays /see Tables by Lederer et al. [9]/ and that there is no EC feeding of the  $^{228}\text{Th}$  ground state. The total transition intensities have been calculated with the use of the theoretical internal conversion coefficients of Hager and Seltzer [6]. The intensity of the 49 transitions not included in the decay scheme corresponds to that of about 11% of the total EC decays. Including of these transitions in the decay scheme would result in a change of the EC branchings and log ft values with respect to those given in Figs 7a and 7b. This, however, could hardly affect the spin and parity assignment to the  $^{228}\text{Pa}$  ground state. We believe also that the qualitative conclusions of section 7.3 on the beta-strength distribution would not be changed.

## 7. DISCUSSION

The properties of the  $^{228}\text{Th}$  levels are discussed in this section in terms of the models developed for the deformed nuclei. For a general presentation of these models the reader may refer to Nathan and Nilsson [10] and Soloviev [11].

### 7.1. Positive-parity states below 1500 keV.

The interpretation of the low-energy  $^{228}\text{Th}$  levels of positive parity is illustrated in Fig. 8.

The ground-state band is shown with four rotational levels. The  $6^+$  level introduced by Arban et al. [1] as uncertain is now well proved by coincidence data. The evidence for the  $8^+$  level is only tentative. The calculations based on the rotational formula, with three parameters determined from the position of the  $2^+$ ,  $4^+$  and  $6^+$  levels, for the  $8^+$  level yield the energy of 824 keV. This is not far from the tentatively given experimental value.

The new level at 1174.5 keV is interpreted as the spin-parity  $5^+$  member of the  $\gamma^-$ -vibrational band. The  $\beta^-$ -vibrational  $0^+$  level, introduced by Lederer et al. [12] at 0.83 MeV, has not been found to be fed in the decay of  $^{228}\text{Pa}$ .

The 1153.6 keV level and the  $\gamma^-$ -vibrational band-head state are linked by the E0 transition<sup>x/</sup>. Hence, for the 1153.6 keV level we have  $KI^\pi = 22^+$ , and therefore this level could be interpreted as a two-phonon  $(\beta + \gamma)^-$ -state. Its energy is, however, significantly lower than the sum of the energies of the  $\beta^-$  - and  $\gamma^-$ -vibrational levels. Similar  $K^\pi = 2^+$  levels have been observed in  $^{230}\text{Th}$  /see Ref. [2] and earlier papers quoted there/ and in  $^{234}\text{U}$  /Björnhelm et al. [14]/.

---

<sup>x/</sup> The E0 character of the 184.5 keV transition was earlier noticed by Björnhelm [13]. Reference should also be made to the recent publication by Horment and Vien [6].

The assignment of  $KI^{\pi} = 44^{+}$  to the 1432.0 keV level has been concluded from the ratios of the E2 reduced probabilities of the transitions to the  $\gamma$ -band. The experimental ratios

$$B(E2, 44^{+} \rightarrow 22^{+}) : B(E2, 44^{+} \rightarrow 23^{+}) : B(E2, 44^{+} \rightarrow 24^{+}) = \\ (1.12 \pm 0.08) : 1 : (0.64 \pm 0.05)$$

are in agreement with the theoretical ones, 1.04: 1 : 0.61, obtained from the Mihailov formula [15] with the parameter  $a = 0.030$ . No agreement is achieved when  $KI^{\pi} = 33^{+}$  is assumed for the decaying state. A possible two-quasiparticle configuration of this state is discussed in section 7.3.

## 7.2. Octupole bands.

The negative-parity states observed in  $^{228}\text{Th}$  below 1500 keV are interpreted as members of the octupole bands (cf. Fig. 9).

The existence of the  $K = 0, 2$  and  $3$  octupole bands observed by Arbman et al. [1] has been confirmed in the present study. The reduced branching ratios for the transitions deexciting these bands are found to be consistent with the adopted interpretation, provided that the analysis is carried out with the use of the Mihailov formula [15].

A new octupole band with  $K = 1$  is proposed to have its first four levels at 951.9, 969, 1015.6 and 1064.1 keV.

The 951.9 keV level. To this level a spin and parity  $1^{-}$  may be assigned only tentatively. The  $1^{-}$  level may be expected to decay to the  $0^{+}$  ground state. The fact that such a transition has not been observed in the  $\gamma$ -ray

spectrum does not necessarily contradict this assignment, since it can be masked by the strong 951.92 keV line of  $^{230}\text{Pa}$ . This level may be interpreted as the head of a new band.

The 969 keV level. The  $K\pi = 12^-$  level at 969 keV is proposed mainly because of its decay to the 396.09 keV  $K\pi = 03^-$  and 327.74 keV  $K\pi = 01^-$  levels. The 573 keV transition appears in coincidence with the 338.32 keV line. We believe that this is a M1 or E2 transition from the 969 keV  $12^-$  level, rather than a K-forbidden E1 transition from the 969.05 keV  $22^+$  level. The 640.6 keV transition is placed between the hypothetical  $2^-$  and the 327.74 keV  $1^-$  levels for the energy-fit reason, without any coincidence support. However, its M1 character is consistent with our interpretation.

The 1015.6 keV level. The existence of this level is well proved by coincidence data. Also it is shown clearly that its parity is negative. This level is a candidate to be interpreted as a  $3^-$  member of the  $K\pi = 1^-$  band.

The 1064.1 keV level. This level could be the  $4^-$  state of the  $K\pi = 1^-$  band, but its existence should be considered as tentative.

If the  $K\pi = 1^-$  band has the level energies as suggested here, it is for the first time possible, anyway to the present author's knowledge, to get some information on the Coriolis interaction of all four one-phonon octupole bands directly from experiment. In the calculations performed it has been necessary to consider several quantities as free parameters: (i) three coupling matrix elements  $A_{01}$ ,  $A_{12}$  and  $A_{23}$  /the subscripts referring to the K values/ and (ii) the unperturbed energy of the

$KI^{\pi} = 33^{-}$  level. The moment-of-inertia parameter  $A$  has been assumed to be the same for all bands. For the sake of simplicity, the relations between  $A$ ,  $A_{01}$  and  $A_{12}$ , derived from the known positions of the  $I = 1$  and  $I = 2$  levels in the  $K = 1$  and  $2$  bands, have been used in the calculations, the small experimental errors being neglected. A fit of the calculated energies to the experimental ones has been performed for the four  $I = 3$  levels. The values of the matrix elements found in this way are listed in Table IV, and compared with the theoretical expectations.

For the parameter values resulting from the best-fit procedure adopted here, the energies of the  $1^{-}$  and  $2^{-}$  levels are reproduced exactly and those of the  $3^{-}$  levels - within  $\pm 0.6$  keV. The agreement between the calculated and experimental energies for the  $4^{-}$  levels is worse. For the  $K = 1$  and  $K = 2$  bands, the calculated energies of the  $4^{-}$  levels are 1039.4 and 1234.2 keV, respectively, which is pretty far from the experimental values.

The experimental energies of the levels of the  $^{228}\text{Th}$  octupole bands are compared in Table V with the theoretical results based on the microscopic-model calculations carried out by different authors.

### 7.3. Distribution of the beta strength in the $^{228}\text{Pa} \rightarrow ^{228}\text{Th}$ decay.

In the considerations of the  $^{228}\text{Pa}$  EC decay given below, the most probable configuration of the Nilsson-model orbitals,  $p\ 530^{\uparrow}$  and  $n\ 752^{\uparrow}$ , has been assumed for the ground state of this nucleus, in agreement with Arbman et al. [1].



The rather low probability /low strength/ observed for the  $\Delta K = 3$  EC decay to the levels of the ground-state band and of the  $K^\pi = 0^-$  octupole band of  $^{228}\text{Th}$  is related to the effect of K forbiddenness. Also, the  $\Delta K = 2$  value for the 1st forbidden transitions to the levels of the possible  $K^\pi = 1^-$  octupole band eliminates all matrix elements, except the unique one, which is compatible with the high limits set for  $\log ft$  values as given in the decay scheme.

The allowed transitions to the gamma-vibrational band, as well as the 1st-forbidden non-unique transitions to the  $K^\pi = 2^-$  and  $3^-$  octupole bands, are not hindered by the K selection rule. To explain the low rate of transitions to the first two of these bands qualitatively, we may refer to the microscopic-model calculations performed by Zheleznova et al. [16]. They show for both collective wave functions a very low contribution of those two-quasiparticle configurations which can presumably participate in the EC transformation. The transition to the  $K^\pi = 3^-$  state at 1450 keV is faster / $\log ft = 7.28$ /. This fact seems to be in a strong disagreement with the results of calculations performed by Block [18] who has found that the  $3^-$  state in question has an almost pure /98.5%/ two-proton configuration,  $(541\downarrow + 642\uparrow)$ , which cannot be fed in the EC decay of  $^{228}\text{Pa}$ . Zheleznova et al. [16] do not give any explicit information on the structure of the  $3^-$  states.

Table VI contains a list of those pure two-quasiparticle states, predicted by the superconductivity model, which have proper configurations from the point of view of their direct EC feeding from the  $^{228}\text{Pa}$  ground state, and which are theoretically predicted at energies below 2.5 MeV.

The ( $752 \uparrow + 761 \uparrow$ ) configuration may possibly be ascribed to the  $4^+$  level observed at 1432 keV. However, identification of other two-quasiparticle states, at higher energy, would be difficult not only because of the lack of complete experimental information on spins, parities,  $\log ft$  values or deexcitation patterns, but also due to the expected level-mixing effects. It has been decided, therefore, to analyse the distribution of the average beta strength rather than probabilities of individual transitions. The energy range of the  $^{228}\text{Th}$  excitations defined by the value of  $Q_{\text{EC}}$  has been divided into  $\Delta E = 0.3$  MeV intervals and for each interval the beta strength

$$S = \frac{1}{\Delta E} \sum \frac{1}{ft}$$

has been calculated. The results are shown in Fig. 10. In the experimental distribution there is a distinct excess of the beta strength in the 1.8 - 2.1 MeV energy interval compared with the theoretical predictions. Perhaps, some two-quasiparticle configurations theoretically expected above 2.5 MeV give an essential contribution to this beta strength excess. This excess could be also an indication of the role of the four-quasiparticle configuration  $n 752 \uparrow$ ,  $n 631 \uparrow$ ,  $p 530 \uparrow$ ,  $p 631 \uparrow$ . Such a state would be fed by a fast, allowed unhindered transition. Admixtures of this four-quasiparticle configuration to some of the even-parity states in the considered energy interval can explain the appearance of the enhancement of the beta decay to these states.

A part of the present studies was performed at the Joint Institute of Nuclear Research in Dubna and the authors should like to thank professor. G.N.Flerov and his co-workers for their hospitality. They are also grateful to Drs. J. Błocki and J. Jastrzębski, Institute of Nuclear Research in Świerk, for discussions.

### REFERENCES

1. Arbmán (E.), Björnholm (S.) and Nielsen (O.B.), Nucl. Phys., 1960, 21, 406.
2. Kurcewicz (W.), Stryczniewicz (K.), Żylicz (J.), Chojnacki (S.), Morek (T.) and Yutlandov (I.), Acta Phys. Polon., 1971, B2, 451.
3. Kaczarowski (R.), Kurcewicz (W.), Płochocki (A.) and Żylicz (J.), Acta Phys. Polon., 1971, B2, 423.
4. Płochocki (A.), Belcarz (E.), Słapa (M.), Szymczak (M.) and Żylicz (J.), Nucl. Instr. and Meth., 1971, 92, 85.
5. Amov (B.G.), Kotlińska (B.) and Kurcewicz (W.), Acta Phys. Polon., 1971, B2, 337.
6. Hager (R.S.) and Seltzer (E.C.), Nuclear Data, 1968, 4, 1.
7. Dalmasso (J.) and Maria (H.), C.R. Acad. Sci., Paris, 1971, B273, 568.
8. Herment (M.) and Vien (Ch.), C.R. Acad. Sci., Paris, 1971, B273, 1058.
9. Lederer (C.M.), Hollander (J.M.) and Perlman (I.), Table of Isotopes, John Wiley, (N.Y.), 1967.

10. Nathan(O.) and Nilsson(S.G.),  
Chap.(X)in "Alpha-, Beta- and Gamma-Ray Spectroscopy",  
edited by K.Siegbahn,  
North-Holland Publishing Company, Amsterdam
11. Soloviev(V.G.),  
Theory of Complex Nuclei,  
"Nauka", Moscow, 1971.
12. Lederer(C.M.),  
Thesis, Report UCRL-11028, 1963.
13. Björnholm(S.),  
private communication.
14. Björnholm(S.), Borggreen(J.), Davis(D.), Hansen(N.J.S.),  
Pedersen(J.) and Nielsen(H.L.),  
Nucl. Phys., 1968, A118, 261.
15. Mihailov(V.M.),  
Izv. Akad. Nauk SSSR, Ser. Fiz., 1966, 30, 1334.
16. Zheleznova(K.M.), Kornejtchuk(A.A.), Soloviev(V.G.),  
Vogel(P.) and Jungklausen(G.),  
JINR Report D-2157, Dubna, 1965.
17. Neergård(K.) and Vogel(P.),  
Nucl. Phys., 1970, A149, 209.
18. Błocki(J.),  
Thesis, Institute of Nuclear Research, Report  
1292/IA/PL, Warsaw, 1971.
19. Błocki(J.) and Kurcewicz(W.),  
Phys. Lett., 1969, 30B, 458.
20. Komov(A.L.), Malov(L.A.) and Soloviev(V.G.),  
JINR Report P4-5126, Dubna 1970.

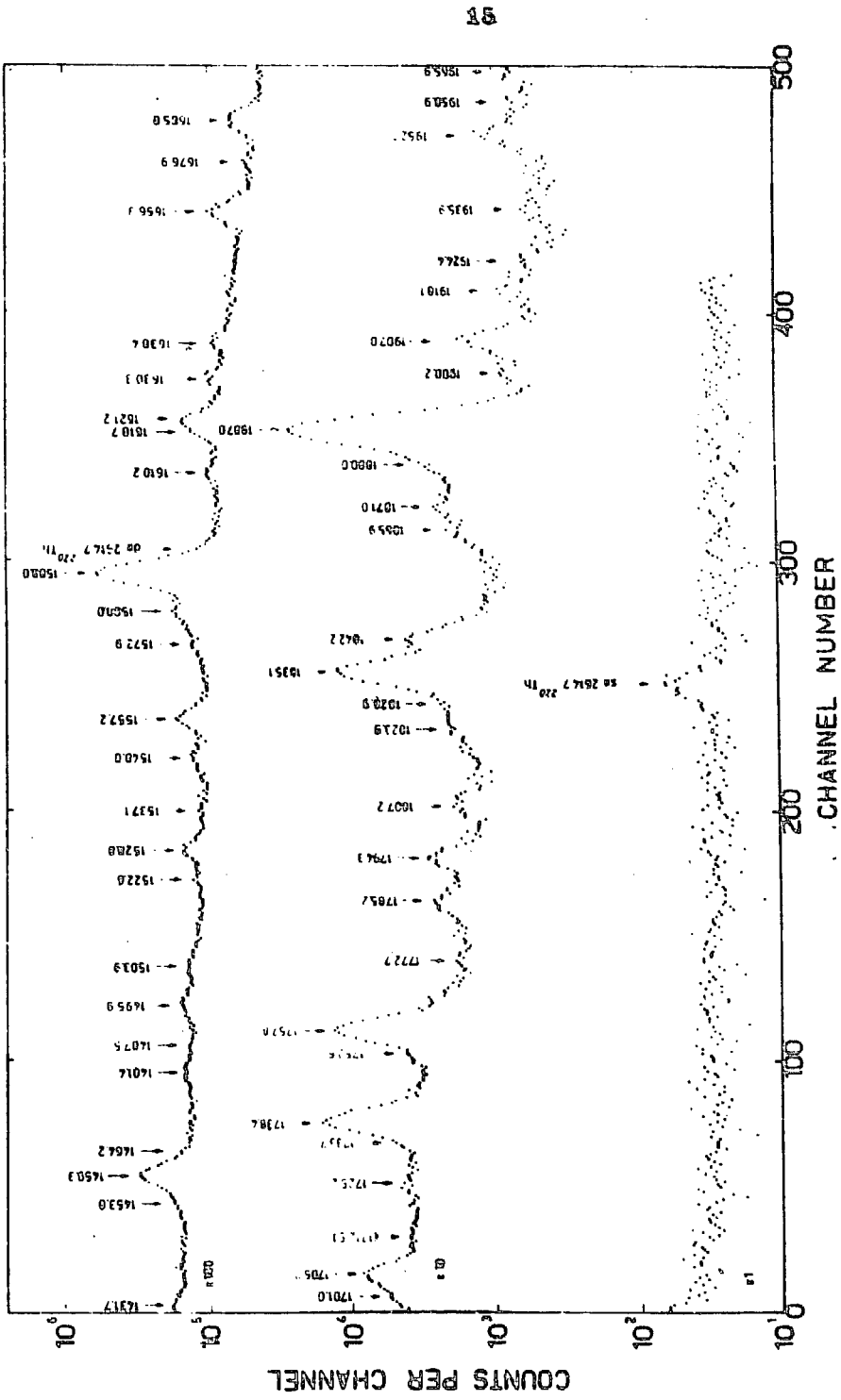


Fig. 1. Gamma-ray spectrum in the energy range above 1400 keV measured using a 33 cm<sup>3</sup> Ge(Li) detector.

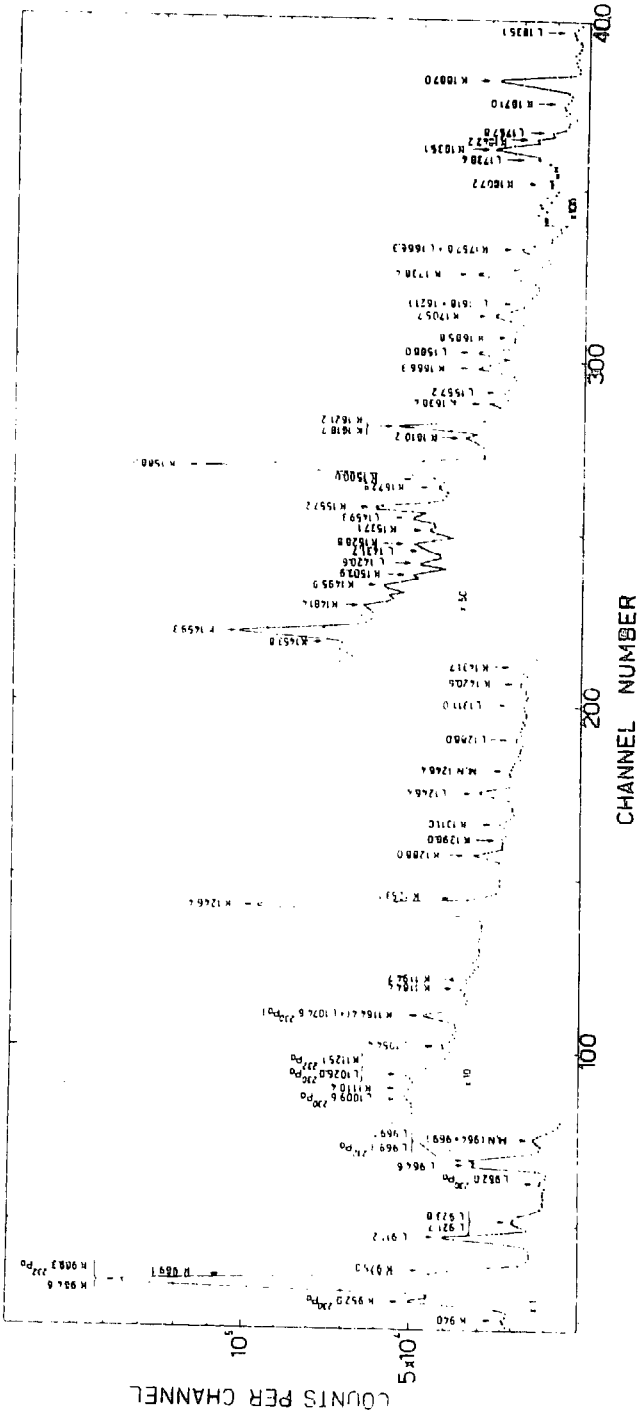


Fig. 2. High-energy part of the spectrum of internal-conversion electrons measured using the  $\beta$  spectrometer with a Si(Li) detector in a homogeneous magnetic field.

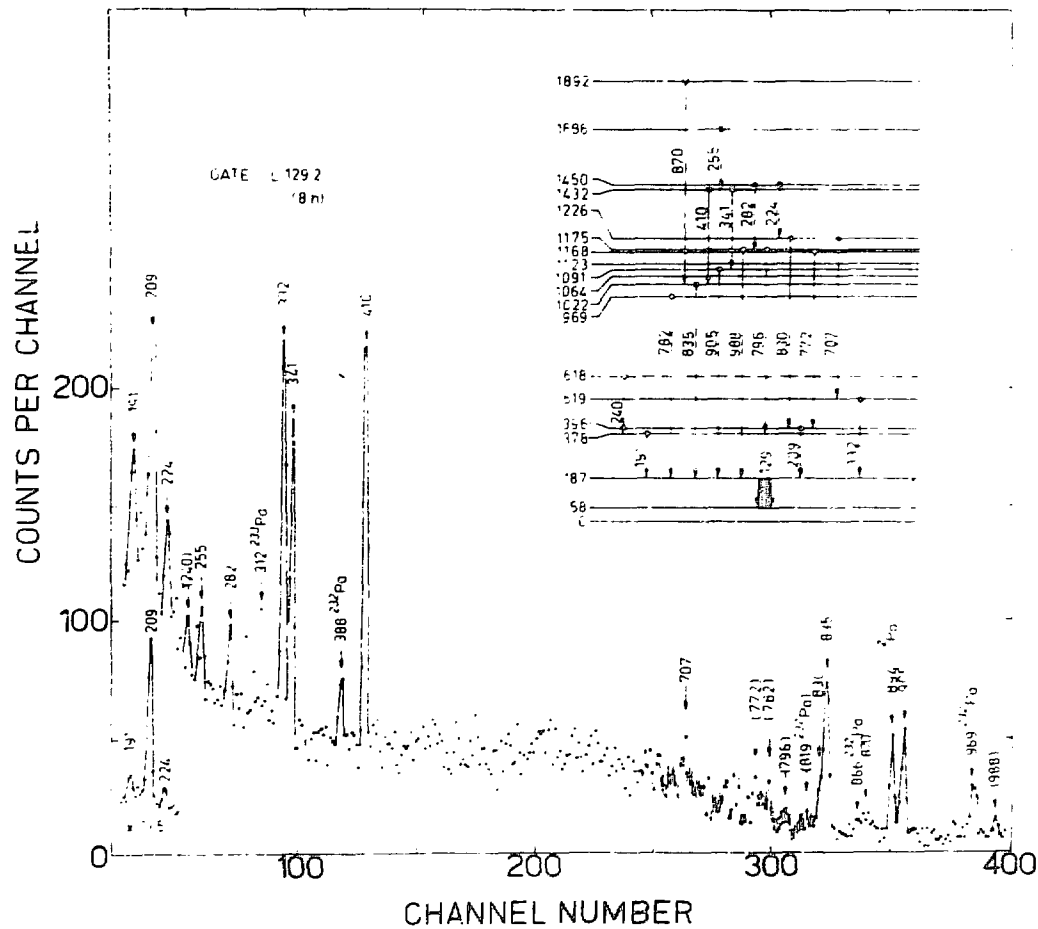


Fig. 3. Gamma-ray spectrum coincident with the L 129.2 internal-conversion line and its interpretation.

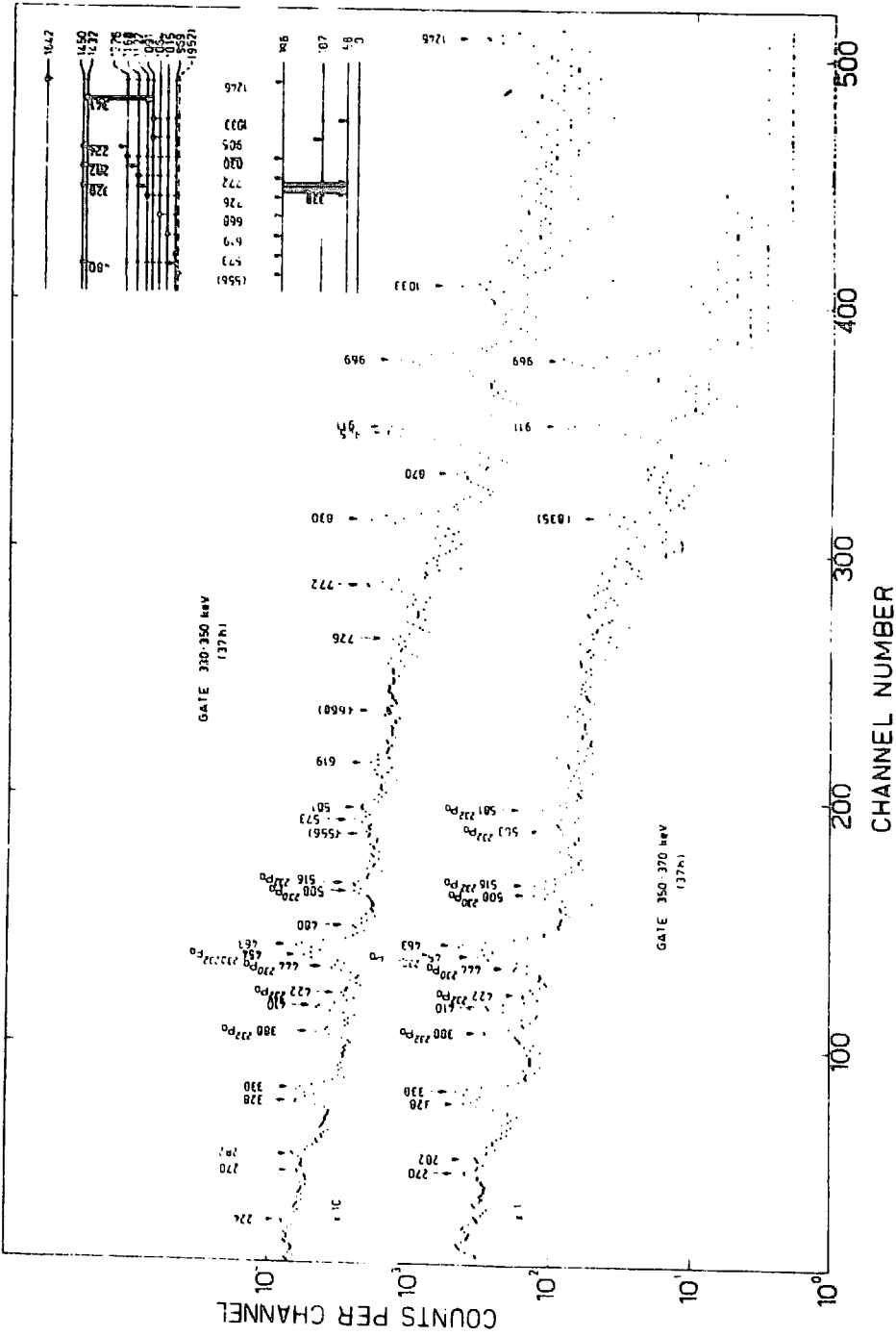


FIG. 4. Gamma-ray spectrum measured in coincidence with the 335.3 keV  $\gamma$ -line and its interpretation. The spectrum coincident with the fraction of the Compton distribution is shown for comparison. The gating transition was taken with a 4.5 cm Ge(Li) detector, the coincident spectrum - with a 13 cm<sup>3</sup> Ge(Li) detector.



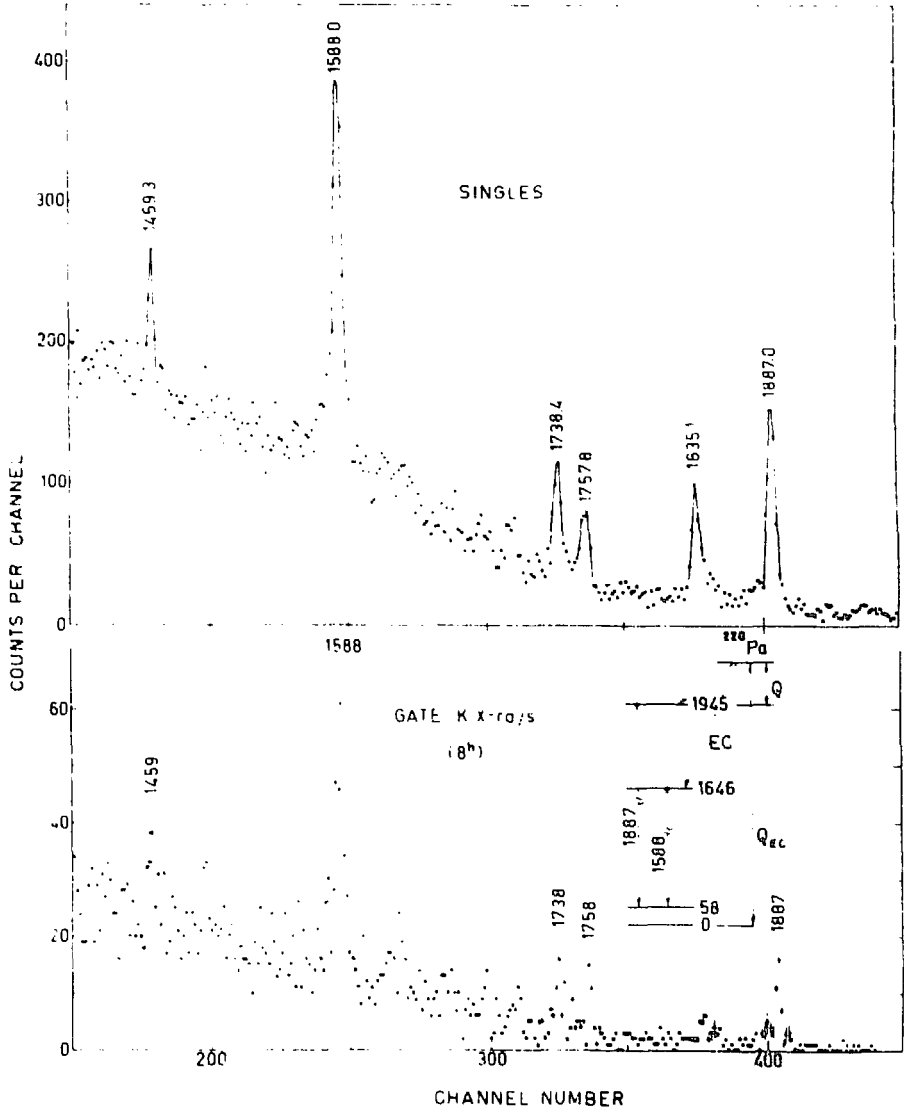


Fig. 5. Section of the singles  $\gamma$ -ray spectrum and the spectrum coincident with K X-rays. Insert: a fragment of the decay scheme.

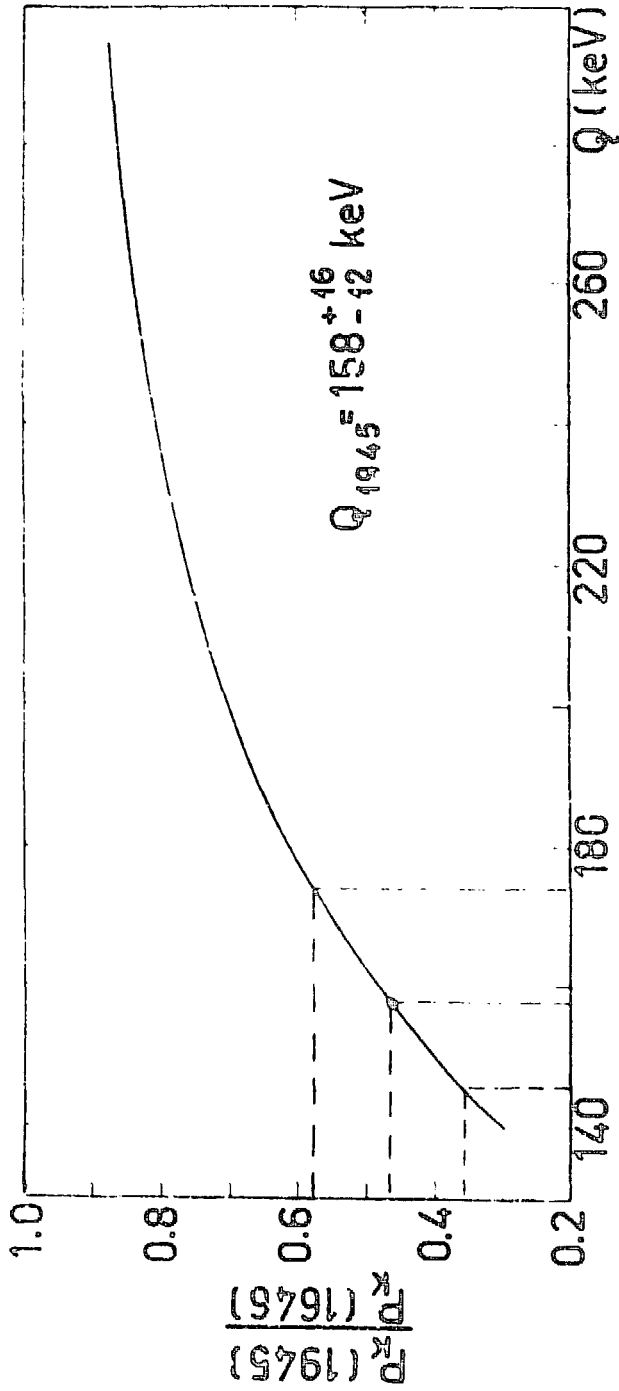


Fig. 6. Dependence of the  $P_K(1945) : P_K(1646)$  ratio as a function of the energy  $Q$  of the EC transition to the 1945 keV level. The experimental value of this ratio, obtained in the coincidence measurements /see Fig. 5/ is also presented.

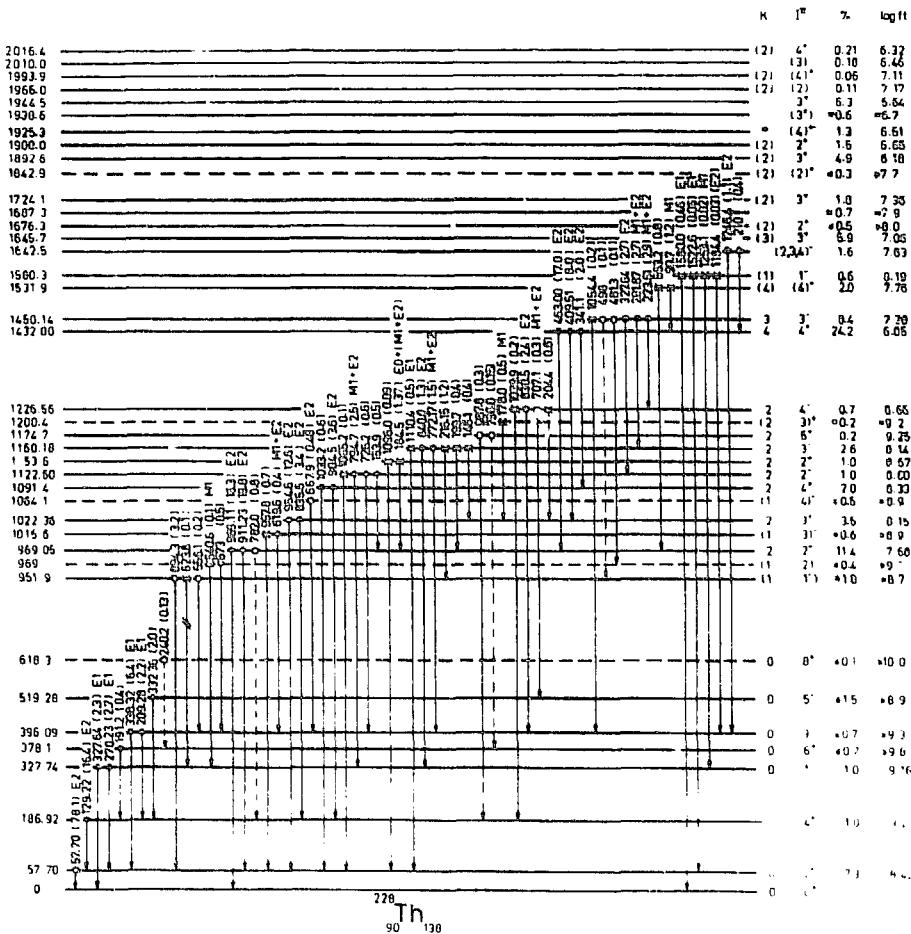


Fig. 7a. The scheme of the  $^{228}\text{Pa}$  decay to the levels in  $^{228}\text{Th}$ . The spacing of close-lying levels is not to scale. The internal transitions whose position in the decay scheme has been established or suggested by coincidence measurements are marked with full and open circles, respectively. Crosses refer to the transitions placed on the basis of the energy fit alone. Transitions placed in two alternative positions are marked with two bars. The intensities /in parentheses/ of the transitions are given in percent of the  $^{228}\text{Pa}$  decays. All energies are in keV.

220 Pa  
 $1^{\pi} = 3^{\pi}$   
 $22^{\pi} = 2103^{\pi}$   
 $EC = 63\%$

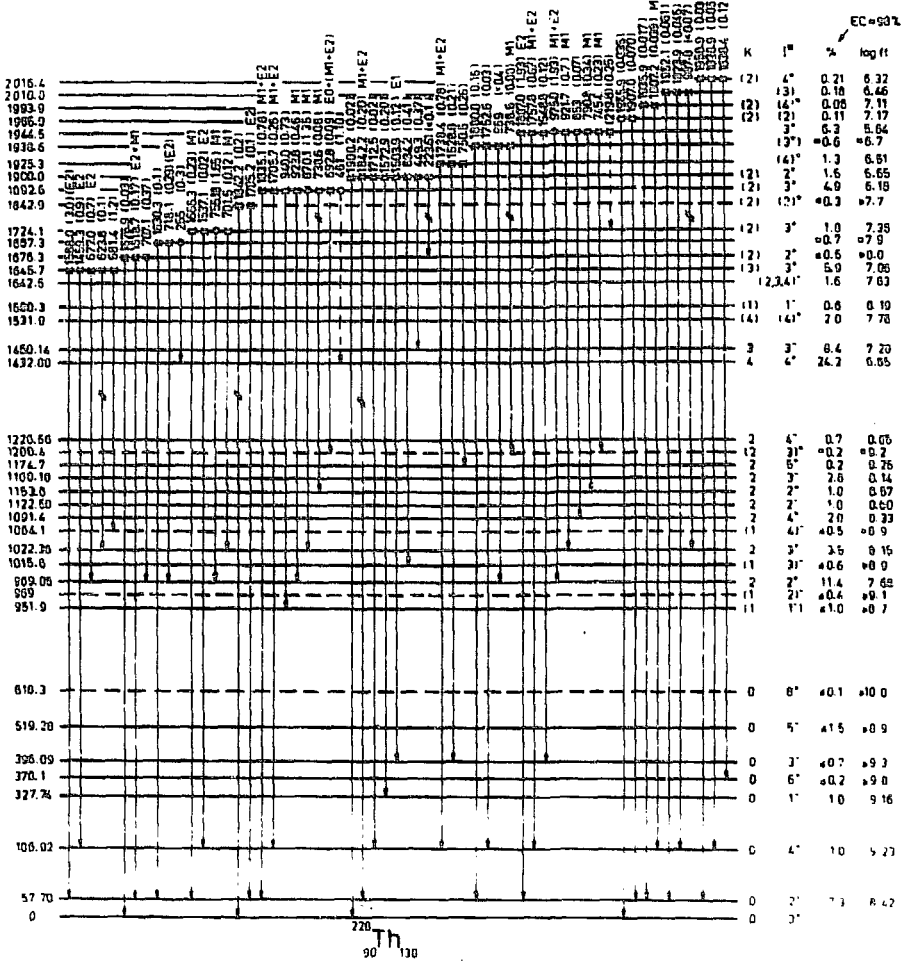


Fig. 7b. The scheme of the  $^{220}\text{Pa}$  decay to the levels in  $^{220}\text{Th}$ . See Fig. 7a for comments.

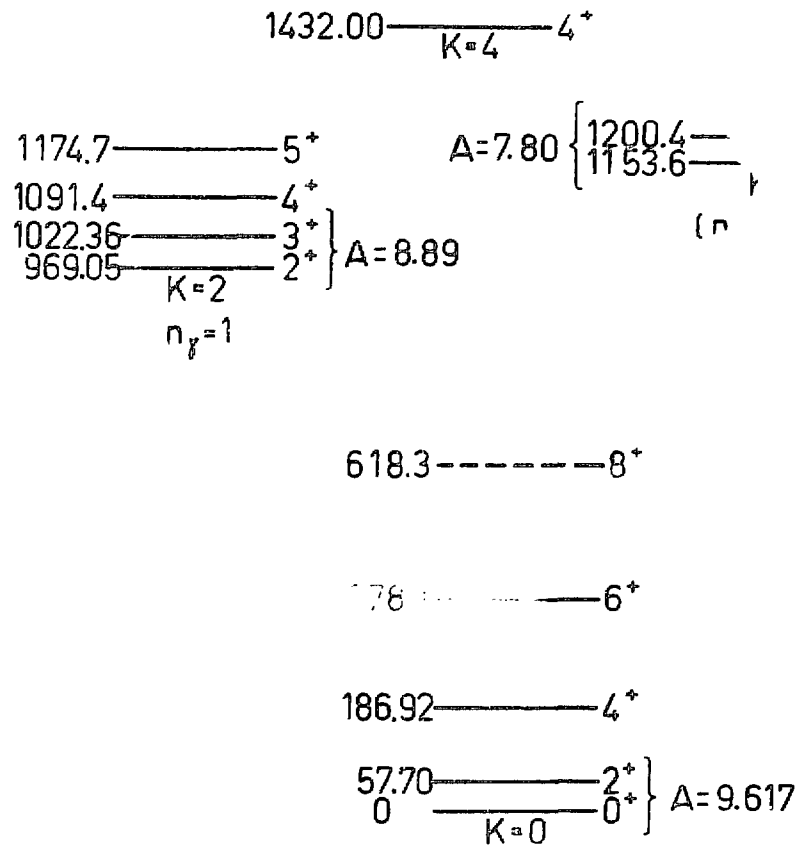


Fig. 8. The interpretation of the  $^{228}\text{Th}$  positive-parity states below 1500 keV. Notation: A - moment-of-inertia parameter in keV,  $n_\beta$  and  $n_\gamma$  - quantum numbers of the  $\beta$  and  $\gamma$  oscillations.

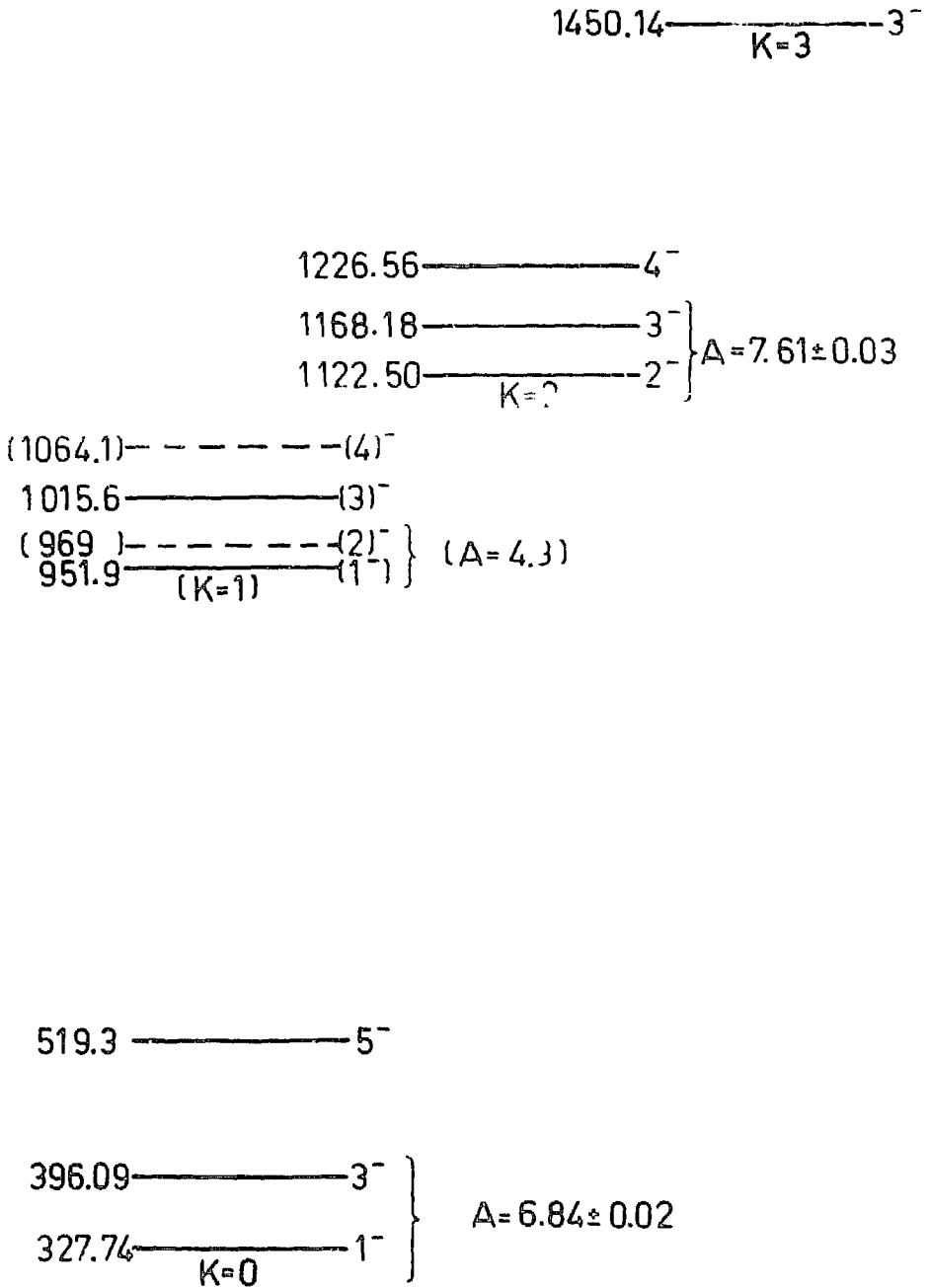


Fig. 9. Octupole bands in  $^{228}\text{Th}$ .  $A$  = moment of-inertia parameter in keV.

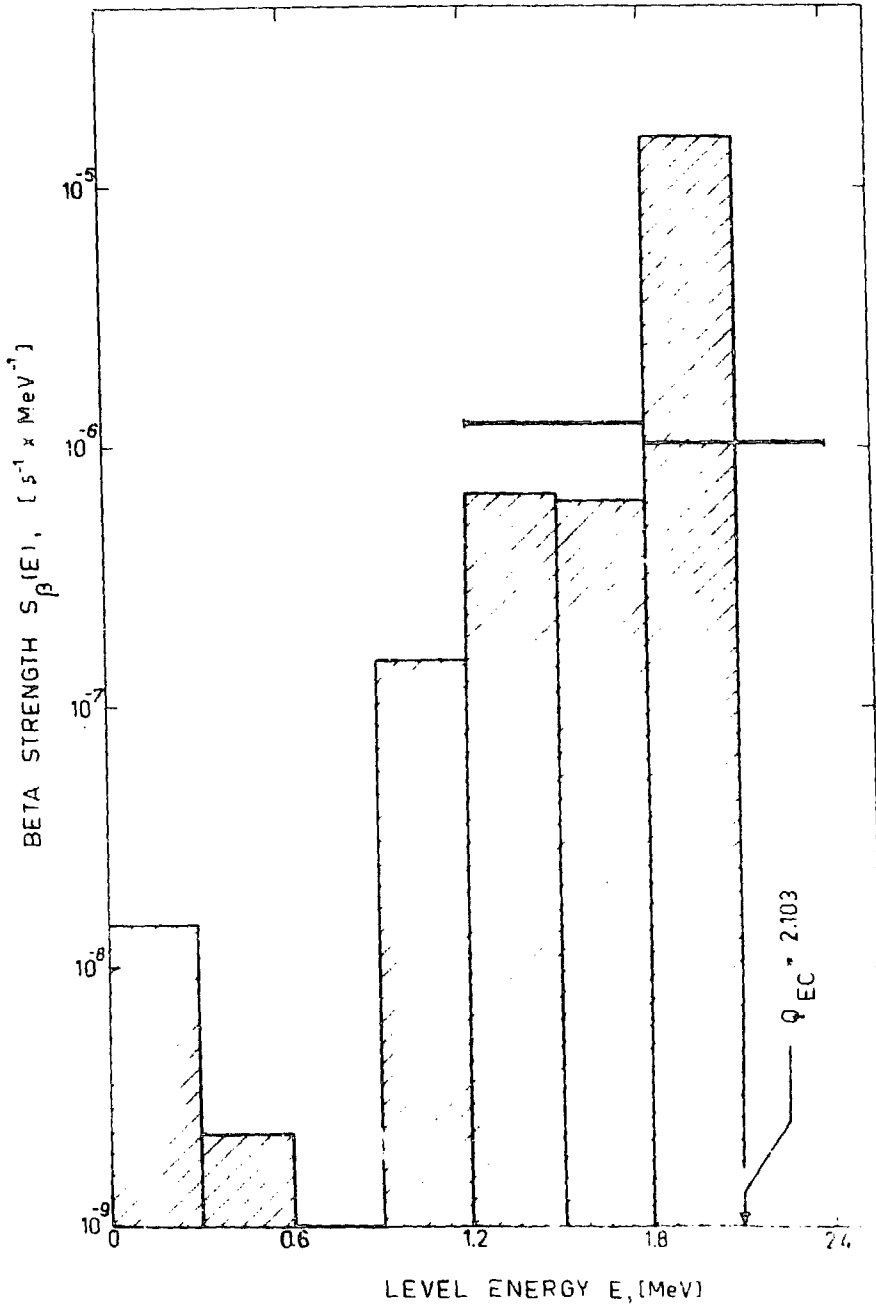


Fig.10. Experimental beta strength distribution for the  $^{228}\text{Pa} \rightarrow ^{228}\text{Th}$  decay. Heavy line /1.2 - 2.4 MeV/ ; distribution calculated for two-quasiparticle states basing on the Table VI data.

TABLE I

Data on internal transitions in  $^{228}\text{Th}$ .

Energy /keV/	Intensity		$\mathcal{L}_K \cdot 10^3$	Multi- polarity	Initial level energy <sup>e)</sup> /keV/
	$\gamma$ rays	K electrons			
57.70 $\pm$ 0.10	87 $\pm$ 14			E2 <sup>a)</sup>	57.70
99.7 $\pm$ 0.3	36 $\pm$ 15			M1 <sup>a)</sup>	1531.9
129.22 $\pm$ 0.10	475 $\pm$ 25			E2 <sup>a)</sup>	186.92
132.0 $\pm$ 0.6	77 $\pm$ 12				
138.3 $\pm$ 0.2	67 $\pm$ 10				
146.1 $\pm$ 0.3	54 $\pm$ 6				1168.18
153.9 $\pm$ 0.3	60 $\pm$ 8				1122.50
178.0 $\pm$ 0.2 <sup>a)</sup>	$\leq$ 14	$\approx 200^{\text{a)}$	$\geq 3400$	M1	1200.4
184.5 $\pm$ 0.2 <sup>a)</sup>	$\leq$ 30	520 $\pm$ 26 <sup>a)</sup>	$\geq 4100$	E0 + (M1+E2)	1153.6
191.2 $\pm$ 0.2	45 $\pm$ 7				378.1
199.7 $\pm$ 0.2	49 $\pm$ 6				1168.18
204.4 $\pm$ 0.2	80 $\pm$ 7				1226.56
209.28 $\pm$ 0.10	278 $\pm$ 25	88 $\pm$ 5 <sup>a)</sup>	75 $\pm$ 9	E1	396.09
210.0 $\pm$ 0.8 <sup>b)</sup>	$\approx 60^{\text{b)}$				1642.5
216.15 $\pm$ 0.10	145 $\pm$ 15				1168.18
(219.8 $\pm$ 0.6)	$\approx 30$				1944.5
223.61 $\pm$ 0.10	153 $\pm$ 13	780 $\pm$ 40 <sup>a)</sup>	1210 $\pm$ 120	M1 + E2	1450.14
(240.2 $\pm$ 0.8 <sup>b)</sup>	$\approx 17^{\text{b)}$				618.3
255 $\pm$ 1 <sup>b)</sup>	50 <sup>b)</sup>				1687.3



TABLE I /continued/

Energy /keV/	Intensity		$\mathcal{L}_K \cdot 10^3$	Multi- polarity	Initial level energy <sup>e)</sup> /keV/
	$\gamma$ rays	K electrons			
270.23 $\pm$ 0.10	350 $\pm$ 17	48 $\pm$ 3 <sup>a)</sup>	33 $\pm$ 3	E1	327.74
278 <sup>a)</sup>	$\leq$ 20	24 $\pm$ 1 <sup>a)</sup>	$\geq$ 290	(M1)	
281.87 $\pm$ 0.10	205 $\pm$ 11	512 $\pm$ 26 <sup>a)</sup>	590 $\pm$ 45	M1 + E2	1450.14
327.64 $\pm$ 0.10	660 $\pm$ 50	116 $\pm$ 6 <sup>a)</sup>	42 $\pm$ 4	E1 and E2	327.74 and 1450.14
332.36 $\pm$ 0.10	262 $\pm$ 24				519.28
338.32 $\pm$ 0.10	850 $\pm$ 50	68 $\pm$ 4 <sup>a)</sup>	19 $\pm$ 2	E1	396.06
341.1 $\pm$ 0.3	257 $\pm$ 20	56 $\pm$ 3 <sup>a)</sup>	52 $\pm$ 5	E2	1432.00
409.51 $\pm$ 0.10	1000 <sup>f)</sup>	216 $\pm$ 11 <sup>a)</sup>	51 $\pm$ 3	E2	1432.00
449.3 $\pm$ 0.6	$\approx$ 50				1900.00
(461 $\pm$ 1) <sup>b)</sup>	$\approx$ 140 <sup>b)</sup>				1892.6
463.00 $\pm$ 0.10	2200 $\pm$ 100	394 $\pm$ 80	42 $\pm$ 9	E2	1432.00
481.3 $\pm$ 0.8	$\approx$ 20				1450.14
(498 $\pm$ 1) <sup>b)</sup>	$\approx$ 100 <sup>b)</sup>				1450.14
525.0 $\pm$ 0.6	30 $\pm$ 10				
547.5 $\pm$ 0.6	20 $\pm$ 5				
556.1 $\pm$ 0.5	30 $\pm$ 6				951.9
563.2 $\pm$ 0.5	110 $\pm$ 30				1531.9
571.1 $\pm$ 0.2	95 $\pm$ 10				
573 $\pm$ 1 <sup>b)</sup>	74 $\pm$ 20 <sup>b)</sup>				969
581.4 $\pm$ 0.2	170 $\pm$ 40				1645.7
589.2 $\pm$ 0.8	$\leq$ 13	1.6 $\pm$ 0.2	$\geq$ 26	M1 + E2	

TABLE I /continued/

Energy /keV/	Intensity		$\propto$ K $\cdot 10^3$	Multi- polarity	Initial level energy <sup>e)</sup> /keV/
	X rays	K electrons			
602.5 $\pm$ 0.8	$\leq$ 10	3.2 $\pm$ 0.4	$\geq$ 66	M1	
614.9 $\pm$ 0.4	16 $\pm$ 4				
619.6 $\pm$ 0.4	50 $\pm$ 20	9.8 $\pm$ 2.0	47 $\pm$ 21	M1 + E2	1015.6
623.8 $\pm$ 0.5	13 $\pm$ 2				951.9 <sup>and/or</sup> 1645.7
640.6 $\pm$ 0.5	10 $\pm$ 5	11 $\pm$ 2	260 $\pm$ 140	M1	969
650.5 $\pm$ 0.4	42 $\pm$ 6				
663.3 $\pm$ 0.6	60 $\pm$ 8	6.4 $\pm$ 1.9	30 $\pm$ 10	M1 + E2	
667.9 $\pm$ 0.6	65 $\pm$ 10	5.8 $\pm$ 1.7	21 $\pm$ 7	E2	1064.1
677.0 $\pm$ 0.4	97 $\pm$ 11	6.6 $\pm$ 1.3	16 $\pm$ 4	E2	1645.7
692.8 $\pm$ 0.8	9 $\pm$ 4	15.5 $\pm$ 2.3	410 $\pm$ 190	E0 + (M1+E2)	1892.6
701.5 $\pm$ 0.5	13 $\pm$ 5	13.5 $\pm$ 2.0	250 $\pm$ 110	M1	1724.1
707.1 $\pm$ 0.2	50 $\pm$ 10	7.0 $\pm$ 2.0	33 $\pm$ 10	M1 + E2	1226.56
718.1 $\pm$ 0.2	40 $\pm$ 2	2.1 $\pm$ 1.0	12 $\pm$ 6	(E2)	1687.3
726.2 $\pm$ 0.8 <sup>b)</sup>	$\approx$ 80 <sup>b)</sup>				1122.50
738.6 $\pm$ 0.6	$\leq$ 15	4.5 $\pm$ 1.0	$\geq$ 71	M1	1892.6 <sup>and/or</sup> 1938.6
745.0 $\pm$ 0.6	$\leq$ 20	8.6 $\pm$ 1.3	$\geq$ 90	M1	1944.5
750.5 $\pm$ 0.5	35 $\pm$ 7				1925.3
755.18 $\pm$ 0.10	210 $\pm$ 14	54.9 $\pm$ 2.8	62 $\pm$ 5	M1	1724.1
772.17 $\pm$ 0.10	198 $\pm$ 11	17.6 $\pm$ 1.4	21 $\pm$ 2	E2 + M1	1168.18
776.5 $\pm$ 0.2	70 $\pm$ 8	3.0 $\pm$ 1.0	10 $\pm$ 3	E2	

TABLE I /continued/

Energy /keV/	Intensity		$\mathcal{L}_K \cdot 10^3$	Multi- polarity	Initial level energy <sup>e)</sup> /keV/
	$\gamma$ rays	K electrons			
(782.0 $\pm$ 0.6) <sup>b)</sup>	$\approx 100$ <sup>b)</sup>				969.05
790.8 $\pm$ 0.3	45 $\pm$ 5	9.1 $\pm$ 1.8	48 $\pm$ 11	M1	1944.5
794.7 $\pm$ 0.2	334 $\pm$ 15	21.3 $\pm$ 3.4	15 $\pm$ 3	E2 + M1	1122.50
(796 $\pm$ 1) <sup>b)</sup>	$\approx 20$ <sup>b)</sup>				1174.7
802.0 $\pm$ 0.5	$\leq 15$	2.8 $\pm$ 0.7	$\geq 44$	M1	
818.0 $\pm$ 0.8	100 $\pm$ 50	3.7 $\pm$ 1.1	8.8 $\pm$ 5.1	E2	
823.5 $\pm$ 1.0	$\approx 40$				
830.5 $\pm$ 0.3	325 $\pm$ 16	18.0 $\pm$ 1.8	13 $\pm$ 2	E2	1226.56
835.5 $\pm$ 0.3	454 $\pm$ 23	22.7 $\pm$ 2.3	12 $\pm$ 2	E2	1022.36
840.0 $\pm$ 0.4	170 $\pm$ 10	6.5 $\pm$ 1.6	9.1 $\pm$ 2.4	E2	1168.18
853 $\pm$ 1	$\leq 10$	2.0 $\pm$ 0.9	$\geq 47$	M1	1944.5
870.1 $\pm$ 0.4	176 $\pm$ 10	26.8 $\pm$ 2.7	38 $\pm$ 4	M1	1892.6
884.2 $\pm$ 0.5	57 $\pm$ 12				1900.0
888.6 $\pm$ 0.5	130 $\pm$ 30	2.9 $\pm$ 0.9	5.3 $\pm$ 2.0	E1	
894.3 $\pm$ 0.5	440 $\pm$ 150				951.9
904.5 $\pm$ 0.3	480 $\pm$ 40	14.4 $\pm$ 2.2	7.1 $\pm$ 1.3	E2	1091.4
911.23 $\pm$ 0.10	2670 $\pm$ 110	100	8.9 <sup>d)</sup>	E2	969.05
921.7 $\pm$ 0.3 <sup>e)</sup>	$\leq 100$	24.1 $\pm$ 3.2 <sup>c)</sup>	$\geq 50$	M1	1944.5
923.8 $\pm$ 0.5 <sup>c)</sup>	$\approx 60$ <sup>b)</sup>	10.8 $\pm$ 3.1 <sup>c)</sup>	$\approx 43$	M1	1892.6
940.0 $\pm$ 0.8	100 $\pm$ 50	1.0 $\pm$ 0.2	2.3 $\pm$ 1.2	E1	1892.6

TABLE I /continued/

Energy /keV/	Intensity		$\mathcal{L}_K \cdot 10^3$	Multi- polarity	Initial level energy $e^-$ /keV/
	$\gamma$ rays	K electrons			
945.6 $\pm$ 0.6	300 $\pm$ 100				
957.6 $\pm$ 0.6	$\approx$ 100				1015.6
964.6 $\pm$ 0.3	1680 $\pm$ 200	68 $\pm$ 27	9.6 $\pm$ 4.0	E2	1022.36
969.11 $\pm$ 0.10	2200 $\pm$ 400	50 $\pm$ 20	5.4 $\pm$ 2.5	E2	969.05 and 1938.6
975.0 $\pm$ 0.3	260 $\pm$ 15	15 $\pm$ 3	14 $\pm$ 3	E2 + M1	1944.5
987.5 $\pm$ 0.2	40 $\pm$ 2				1174.7 and 2010.0
1018.6 $\pm$ 0.3	35 $\pm$ 5				
1033.2 $\pm$ 0.3	60 $\pm$ 5				1091.4
1039.9 $\pm$ 0.3	28 $\pm$ 4				1226.56
1046.1 $\pm$ 0.6	6 $\pm$ 2				
1054.4 $\pm$ 0.5	23 $\pm$ 6				1450.14
1065.2 $\pm$ 0.5	13 $\pm$ 1				1122.50
1070.2 $\pm$ 0.5	19 $\pm$ 4				
1096.0 $\pm$ 0.8	5 $\pm$ 2				1153.6
1103.9 $\pm$ 0.8	3 $\pm$ 1				
1110.4 $\pm$ 0.2	72 $\pm$ 3	0.55 $\pm$ 0.11	1.8 $\pm$ 0.4	E1	1168.16
1118.6 $\pm$ 0.6	7 $\pm$ 1				
1164.4 $\pm$ 0.6	12 $\pm$ 1	0.70 $\pm$ 0.07	14 $\pm$ 2	E2 + M1	
1184.4 $\pm$ 0.6	4 $\pm$ 2	0.22 $\pm$ 0.06	13 $\pm$ 7	E2, M1	1580.3
1194.7 $\pm$ 1.0	3 $\pm$ 1	0.15 $\pm$ 0.05	12 $\pm$ 6	E2, M1	

TABLE I /continued/

Energy /keV/	Intensity		$\propto$ K $\cdot 10^3$	Multi- polarity	Initial level energy <sup>e)</sup> /keV/
	$\gamma$ rays	K electrons			
1237.7 $\pm$ 0.6	14 $\pm$ 2				
1246.4 $\pm$ 0.2	150 $\pm$ 7	2.9 $\pm$ 0.3 <sup>c)</sup>	4.6 $\pm$ 0.5	E2	1642.5
1253.1 $\pm$ 0.6	3 $\pm$ 1	0.29 $\pm$ 0.08 <sup>c)</sup>	23 $\pm$ 10	M1	1580.3
1273.0 $\pm$ 0.6	13 $\pm$ 2				
1288.0 $\pm$ 0.4	20 $\pm$ 1	0.72 $\pm$ 0.07	8.5 $\pm$ 1.0	E2 + M1	
1298.0 $\pm$ 0.4	19 $\pm$ 2	0.21 $\pm$ 0.07	2.6 $\pm$ 0.9	E1 + M2	
1311.0 $\pm$ 0.6	9 $\pm$ 3	0.26 $\pm$ 0.06	6.9 $\pm$ 2.7	E2 + M1	
1420.6 $\pm$ 0.6	16 $\pm$ 1	0.34 $\pm$ 0.08	5.1 $\pm$ 1.2	E2	
1431.7 $\pm$ 0.6	23 $\pm$ 2	0.51 $\pm$ 0.09	5.3 $\pm$ 1.1	E2	
1453.8 $\pm$ 0.6	20 $\pm$ 1	0.13 $\pm$ 0.06	1.5 $\pm$ 0.7	E1	
1459.3 $\pm$ 0.2	120 $\pm$ 5	1.73 $\pm$ 0.30 <sup>c)</sup>	3.4 $\pm$ 0.6	E2	1645.7
1464.2 $\pm$ 0.2	10 $\pm$ 5				
1481.4 $\pm$ 0.6	15 $\pm$ 1	0.30 $\pm$ 0.10	4.7 $\pm$ 1.6	E2	
1497.5 $\pm$ 0.6	$\approx$ 9				
1495.9 $\pm$ 0.4	28 $\pm$ 2	0.35 $\pm$ 0.10	3.0 $\pm$ 1.0	E1, E2	
1503.9 $\pm$ 0.6	16 $\pm$ 1	0.16 $\pm$ 0.07	2.4 $\pm$ 1.1	E1	1900.0
1522.6 $\pm$ 0.6	5 $\pm$ 1				1580.3
1524.8 $\pm$ 0.4	29 $\pm$ 2	0.40 $\pm$ 0.12	3.3 $\pm$ 1.1	E1, E2	1925.3
1537.1 $\pm$ 0.8	2 $\pm$ 1	0.26 $\pm$ 0.07	2.9 $\pm$ 1.5	E2	1724.1
1548.5 $\pm$ 0.6	16 $\pm$ 1				1944.5

TABLE I /continued/

Energy /keV/	Intensity		$\mathcal{L}_K \cdot 10^3$	Multi- polarity	Initial level energy <sup>e)</sup> /keV/
	$\gamma$ rays	K electrons			
1557.2 $\pm$ 0.3	46 $\pm$ 2	1.1 $\pm$ 0.2	5.7 $\pm$ 1.2	E2 + M1	
1572.9 $\pm$ 0.6	28 $\pm$ 5	0.34 $\pm$ 0.11	2.8 $\pm$ 1.0	E1, E2	1900.0
1580.0 $\pm$ 0.4	63 $\pm$ 6	0.45 $\pm$ 0.14	1.7 $\pm$ 0.5	E1	1580.3
1588.0 $\pm$ 0.2	405 $\pm$ 18	4.1 $\pm$ 0.6 <sup>c)</sup>	2.4 $\pm$ 0.4	(E2)	1645.7
1610.2 $\pm$ 0.4	12 $\pm$ 1	0.58 $\pm$ 0.13	11 $\pm$ 3	M1	
1618.7 $\pm$ 0.4	23 $\pm$ 3	0.46 $\pm$ 0.15	4.7 $\pm$ 1.6	E2 + M1	1676.3
1621.2 $\pm$ 0.4	43 $\pm$ 4	1.3 $\pm$ 0.3	7.2 $\pm$ 1.7	M1	
1630.3 $\pm$ 0.4	17 $\pm$ 2				1687.3
1638.4 $\pm$ 0.4	16 $\pm$ 2	0.23 $\pm$ 0.07	3.4 $\pm$ 1.1	E2	2016.4
1666.3 $\pm$ 0.2	31 $\pm$ 2	1.2 $\pm$ 0.3 <sup>c)</sup>	9.2 $\pm$ 2.4	M1	1724.1
1676.9 $\pm$ 0.6	5 $\pm$ 1				1676.3
1685.8 $\pm$ 0.4	24 $\pm$ 2	0.33 $\pm$ 0.12	3.2 $\pm$ 1.2	E2	
1701.0 $\pm$ 0.6	10 $\pm$ 1				
1705.7 $\pm$ 0.4	36 $\pm$ 2	0.9 $\pm$ 0.2	5.9 $\pm$ 1.3	E2 + M1	1892.6
(1712.5 $\pm$ 0.6)	$\approx$ 2				1900.0
1725.2 $\pm$ 0.6	4 $\pm$ 1				
1733.7 $\pm$ 0.8	7 $\pm$ 2				
1738.4 $\pm$ 0.2	106 $\pm$ 5	2.60 $\pm$ 0.26 <sup>c)</sup>	5.8 $\pm$ 0.7	E2 + M1	1925.3
1752.6 $\pm$ 0.6	5 $\pm$ 1				1938.6
1757.8 $\pm$ 0.2	90 $\pm$ 5	1.50 $\pm$ 0.30 <sup>c)</sup>	3.9 $\pm$ 0.8	E2 + M1	1944.5

TABLE I /continued/

Energy /keV/	Intensity		$\mathcal{L}_K \cdot 10^3$	Multipo- larity	Initial level energy <sup>e)</sup> /keV/
	$\gamma$ rays	K electrons			
1772.7 $\pm$ 0.6	5 $\pm$ 1				
1785.2 $\pm$ 0.3	14 $\pm$ 1	0.28 $\pm$ 0.14	4.7 $\pm$ 2.4	E2 + M1	1842.9
1794.3 $\pm$ 0.3	15 $\pm$ 1				
1807.2 $\pm$ 0.5	5.4 $\pm$ 0.4	0.16 $\pm$ 0.08	7.0 $\pm$ 3.6	E2 + M1	1993.9
1823.9 $\pm$ 0.8	6 $\pm$ 1				2010.0
1828.9 $\pm$ 0.8	9 $\pm$ 2				2016.4
1835.1 $\pm$ 0.2	106 $\pm$ 6	1.56 $\pm$ 0.23 <sup>c)</sup>	3.5 $\pm$ 0.6	E2 + M1	1892.6
1842.2 $\pm$ 0.3	27 $\pm$ 2	0.60 $\pm$ 0.20 <sup>o)</sup>	5.2 $\pm$ 1.8	E2 + M1	1900.0 and/or 1842.9
1865.9 $\pm$ 0.6	8 $\pm$ 1				$\frac{1}{2}$
1871.0 $\pm$ 0.6	15 $\pm$ 2	0.18 $\pm$ 0.09	2.8 $\pm$ 1.4	(E2)	
1880.0 $\pm$ 0.8	23 $\pm$ 2				1938.6
1887.0 $\pm$ 0.2	260 $\pm$ 15	2.97 $\pm$ 0.45 <sup>o)</sup>	2.7 $\pm$ 0.4	E2	1944.5
1900.2 $\pm$ 0.6	2.6 $\pm$ 0.3				1900.0
1907.0 $\pm$ 0.4	9.8 $\pm$ 0.5				1965.0
1918.1 $\pm$ 0.6	2.8 $\pm$ 0.3				
1924.4 $\pm$ 0.6	1.4 $\pm$ 0.3				
1935.9 $\pm$ 0.6	2.4 $\pm$ 0.3				1993.9
1952.1 $\pm$ 0.6	8.5 $\pm$ 0.6				2010.0
1958.9 $\pm$ 0.8	3.6 $\pm$ 0.5				2016.4
1965.9 $\pm$ 0.8	4.8 $\pm$ 0.6				1965.0

- a) Data from Ref. [1]; K-electron intensities are renormalized by the present authors and assumed to be accurate within about 5% /see caption to Table I in Ref. [1]/.
- b) Data from our coincidence measurements.
- c) Data from Ref. [5].
- d) Based on assumption of E2 multipolarity for the 911.23 keV transition.
- e) For the transitions placed in the decay scheme /see Figs 7a and 7b/.
- f) The intensity of 1000 units corresponds to 7.4% of the  $^{228}\text{Pa}$  decay rate.



TABLE II  
Results of the  $e\gamma$  coincidence studies

Selected conversion line	Energies /keV/ and intensities /in brackets/ of coincident $\gamma$ lines
L57.7	209 (250 $\pm$ 50) , 270 (254 $\pm$ 57) , 282 (160 $\pm$ 60) , 332 (290 $\pm$ 70) , 338 (890 $\pm$ 100) , 410 (950 $\pm$ 110) , 463 (1330 $\pm$ 150) , 4987 ( $\approx$ 100) , 830 ( $\approx$ 250) , 835 and/or 840 ( $\approx$ 390) , 894? ( $\approx$ 150) , 905 ( $\approx$ 420) , 911 ( $\equiv$ 2670) , 965 (1780 $\pm$ 330)
L129.3	191 (41 $\pm$ 15) , 209 (264 $\pm$ 23) , 224 (39 $\pm$ 12) , 240? ( $\approx$ 17) , 255 (32 $\pm$ 11) , 282 (42 $\pm$ 14) , 332 (240 $\pm$ 25) , 341 (205 $\pm$ 24) , 410 (360 $\pm$ 41) , 707 (105 $\pm$ 47) , 772? ( $\approx$ 110) , 782? ( $\approx$ 105) , 796? ( $\approx$ 20) , 830 (180 $\pm$ 85) , 835 ( $\equiv$ 450) , 870 ( $\approx$ 50) , 905 (390 $\pm$ 65) , 988? ( $\approx$ 90)

TABLE III  
Results of the  $\gamma$   $\gamma$  coincidence studies

Selected energy interval /keV/	Selected $\gamma$ lines /keV/	Energies /keV/ and intensities /in brackets/ of coincident $\gamma$ lines
260 - 280	270	282(71 $\pm$ 27) , 328(312 $\pm$ 62) , 795( $\equiv$ 334) , 840(153 $\pm$ 44)
330 - 350	338	224(40 $\pm$ 8) , 282(35 $\pm$ 12) , 328(26 $\pm$ 13) , 480(36 $\pm$ 17) , 556? $\approx$ 50) , 573(74 $\pm$ 20) , 619(31 $\pm$ 16) , 668? $\approx$ 50) , 726(51 $\pm$ 20) , 772( $\equiv$ 198) , 830(250 $\pm$ 40) , 870(24 $\pm$ 14) , 1246(100 $\pm$ 36) 905( $\equiv$ 480) , 1033(120 $\pm$ 50)
400 - 420	410	129(174 $\pm$ 34) , 210(65 $\pm$ 20) , 461? $\approx$ 50) , 520(60 $\pm$ 36) , 835(470 $\pm$ 95) , 965( $\equiv$ 1680)
790 - 810	795	270( $\equiv$ 350) , 328(820 $\pm$ 250)
900 - 920	905 912	341(124 $\pm$ 30) 154(53 $\pm$ 21) , 328(47 $\pm$ 25) , 463( $\equiv$ 2200) , 481? $\approx$ 60) , 707( $\approx$ 20) , 755(290 $\pm$ 70) , 923( $\approx$ 60) , 975(180 $\pm$ 60)

TABLE IV

Matrix elements of the Coriolis interaction  
between octupole bands /in keV/

$A_{K,K+1}$	Experiment	theory		
	a)	b)	c)	d)
$A_{01}$	31.5	32.0	42.3	7.2
$A_{12}$	21.5	29.2	41.9	44.1
$A_{23}$	35.5	22.6	-	60.4

- a) From the analysis of the level-energy spacings.  
The inertial parameter  $A = 8.34$  keV.
- b) The spherical-limit values calculated according  
to the formula given by Neergård and Vogel [17].
- c) Based on microscopic calculations by Zheleznova  
et al. [16].
- d) Based on microscopic calculations by Błocki [18].

TABLE V

Energy levels of complete  
bands in  $^{228}\text{Th}$

K	$I^\pi$	Energy (keV)				
		Experiment this work	ref. [16]	ref. [19]	ref. [17]	ref. [20]
0	$1^-$	328	350	620	360	460
	$3^-$	396			400	
	$5^-$	519				
1	$1^-$	952	1110	1020	880	1100
	$2^-$	969			890	
	$3^-$	1016			930	
	$4^-$	1064				
2	$2^-$	1122	1600	1160	1130	1400
	$3^-$	1168			1200	
	$4^-$	1227				
3	$3^-$	1450		1530	1420	

TABLE VI

Two-quasiparticle levels in  $^{228}\text{Th}$  fed by allowed and first forbidden EC decay of  $^{228}\text{Pa}$

Two-quasiparticle states			log ft /estimated/
Configuration	Energy /MeV/	Jpin and parity	
$nn(752\uparrow + 631\uparrow)$	1.31	$4^-$	7.2
$nn(752\uparrow + 761\uparrow)$	1.44	$4^+$	6.5
$nn(752\uparrow + 770\uparrow)$	1.71	$3^+$	6.5
$nn(752\uparrow + 640\uparrow)$	1.76	$3^-$	7.2
$nn(752\uparrow + 501\downarrow)$	1.97	$2^+$	6.5
$nn(752\uparrow - 631\downarrow)$	2.11	$2^-$	6.5

Energies calculated by Blocki and Kurcewicz

/unpublished/. The version of the superconductivity model used in these calculations has been earlier described in Refs.

[18] and [19].

